Rapid Communications

Dynamical formation of the unitary Bose gas

V. E. Colussi,* S. Musolino, and S. J. J. M. F. Kokkelmans
Eindhoven University of Technology, P.O. Box 513, 5600 MB Eindhoven, The Netherlands

(Received 17 May 2018; published 2 November 2018)

We study the structure of a Bose-condensed gas after quenching interactions to unitarity. Using the method of cumulants, we decompose the evolving gas in terms of clusters. Within the quantum depletion we observe the emergence of two-body clusters bound purely by many-body effects, scaling continuously with the atomic density. As the unitary Bose gas forms, three-body Efimov clusters are first localized and then sequentially absorbed into the embedded atom-molecule scattering continuum of the surrounding depletion. These results highlight the interplay of quantum depletion and evolving scaling laws in the formation of the unitary Bose gas.

DOI: 10.1103/PhysRevA.98.051601

Introduction. Precision control of external magnetic fields allows ultracold Bose gas experiments to tune interactions, characterized by the s-wave scattering length a. Via Feshbach resonances [1], experiments have accessed the degenerate unitary regime $n|a|^3 \to \infty$ with atomic density n, beating per-particle losses scaling as $\dot{n}/n \sim n^2a^4$ by diabatically quenching the scattering length to resonance ($|a| \to \infty$) [2–4]. The insensitivity of unitary quantum gases to diverging microscopic length scales extends their properties to seemingly unrelated strongly correlated physical systems, such as the inner crust of neutron stars and the quark-gluon plasma [5]. This predictive power is due to the intrinsic scale invariance of these unitary systems [6]. Strong experimental evidence for two-component unitary Fermi gases [7,8] supports a universal thermodynamics based solely on continuous power laws of the atomic density derived "Fermi" scales $k_\mathrm{n} = (6\pi^2 n)^{1/3}$, $E_\mathrm{n} = \hbar^2k_\mathrm{n}^2/2m$, and time $t_\mathrm{n} = \hbar/E_\mathrm{n}$ where m is the atomic mass [9]. The scaling behavior of the unitary Bose gas is complicated by the finite-size and discrete-scaling properties of three-body bound Efimov states [10,11], introducing a complex scaling dimension [6]. A full characterization of the quasiequilibrium state of the unitary degenerate Bose gas observed experimentally [2,4] remains an open question, limiting insight into other strongly correlated many-body systems.

These difficulties are symptoms of an undeveloped picture of few-body physics in the evolving many-body background and their manifestations in system properties on Fermi timescales. Recently, the problem of merging the Efimov effect and a many-body background has received attention in the related context of impurities immersed in static bosonic [12–16] or fermionic [17–22] media. However, the dynamical nature of quench experiments poses an additional theoretical challenge. Initially, the quench disturbs short-range physics in the gas, inducing ballistic correlation waves [23] and sequential clustering [24,25]. Recently measured per-particle loss rates for quenched unitary Bose gases scaling continuously over a range of atomic densities suggest that Efimov physics plays only a minor role for this observable [3,4]. However, over a wider range of atomic densities, preliminary loss-rate measurements [26] and theoretical results [25] indicate a log-periodic oscillation of the loss rate with a density period set by the Efimov spacing $e^{3\pi/s_0} \approx 22.7^3$ where $s_0 \approx 1.00624$ is a universal constant for three identical bosons [10]. These results parallel oscillatory loss-rate predictions in the nondegenerate regime [27].

In this Rapid Communication, we explore the composition of a Bose condensate quenched to unitarity. Our model applies to broad, entrance-channel dominated Feshbach resonances that are well approximated by short-range single-channel interactions [1]. This system has been realized experimentally in Refs. [2,3] using ^{85}Rb and in Ref. [4] using ^{39}K. Using the method of cumulants, we derive two- and three-body Schrödinger equations including density effects. These yield the evolving spectrum of bound two- and three-body clusters. We map out the dynamical and density scaling properties of the bound cluster spectrum and comment on manifestations in system properties.

Cumulant equations. Our quantitative many-body theory of the Bose-condensed gas quenched to unitarity is built from the cumulant expansion, which classifies correlated particle clusters within an interacting many-body system [28,29]. The second-order cumulant expansion yields the Hartree-Fock-Bogoliubov equations (HFB) [30]. These equations may be systematically extended to higher order, yielding few-particle cluster kinetics that can be used to explore strongly interacting few-body physics like the Efimov effect. In terms of the bosonic annihilation and creation operators, $\hat{a}_\mathbf{k}$ and $\hat{a}_\mathbf{k}^\dagger$ respectively, for a particle of momentum $\hbar\mathbf{k}$, cumulants are defined from normal-ordered expectation values

$$\left\langle \prod_{i=1}^{l} \hat{a}_{\mathbf{k}_i}^\dagger \prod_{j=1}^{m} \hat{a}_{\mathbf{q}_j} \right\rangle_c \equiv (-1)^m \prod_{i=1}^{l} \frac{\partial}{\partial x_i} \prod_{j=1}^{m} \frac{\partial}{\partial y_j^*} \times \ln \left\langle e^{\sum_{i=1}^{l} x_i \hat{a}_{\mathbf{k}_i}^\dagger} e^{-\sum_{j=1}^{m} y_j^* \hat{a}_{\mathbf{q}_j}} \right\rangle \Big|_{\mathbf{x},\mathbf{y}=0}, \quad (1)$$

in terms of complex-valued x_i and y_j. For uniform systems, the set of relevant cumulants in the above equation are restricted such that $\sum_{i=1}^{l} \mathbf{k_i} = \sum_{j=1}^{m} \mathbf{q_j}$. To model the condensate and excitations, we make the Bogoliubov approximation [30], decomposing operators as $\hat{a}_\mathbf{k} = \psi_\mathbf{k} + \delta\hat{a}_\mathbf{k}$ in terms

*Corresponding author: colussiv@gmail.com

of coherent state amplitude $\langle \hat{a}_{\mathbf{k}} \rangle = \psi_0 \delta_{\mathbf{k},0}$ and fluctuations $\langle \delta \hat{a}_{\mathbf{k}\neq 0} \rangle = 0$. This is justified provided excited modes are not macroscopically occupied. Isolating the condensate in the first-order cumulant ψ_0, we truncate the cumulant expansion at second order, which describes genuine two-excitation correlations. This includes also the one-body $\rho_{\mathbf{k}} \equiv \langle \hat{a}^\dagger_{\mathbf{k}} \hat{a}_{\mathbf{k}} \rangle_c$ and pairing $\kappa_{\mathbf{k}} \equiv \langle \hat{a}_{\mathbf{k}} \hat{a}_{-\mathbf{k}} \rangle_c$ density matrices for excitations. We utilize a single-channel many-body Hamiltonian applicable in the vicinity of a broad Feshbach resonance

$$\hat{H} = \sum_{\mathbf{k}} \frac{\hbar^2 k^2}{2m} \hat{a}^\dagger_{\mathbf{k}} \hat{a}_{\mathbf{k}} + \frac{g}{2} \sum_{\mathbf{p},\mathbf{p}',\mathbf{q}} \zeta(\mathbf{p} - \mathbf{p}' + 2\mathbf{q}) \times \zeta^*(\mathbf{p} - \mathbf{p}') \hat{a}^\dagger_{\mathbf{p}+\mathbf{q}} \hat{a}^\dagger_{\mathbf{p}'-\mathbf{q}} \hat{a}_{\mathbf{p}} \hat{a}_{\mathbf{p}'}. \tag{2}$$

At energies close to a two-body bound state, the two-body T matrix becomes separable [31], and we use a nonlocal separable pairwise potential, $\hat{V} = g|\zeta\rangle\langle\zeta|$. We employ a step-function form factor $\zeta(\mathbf{k}) = \Theta(\Lambda - |\mathbf{k}|/2)$, which has been previously used to study Efimov states in vacuum (cf. Ref. [32]). The s-wave interaction strength g is calibrated to reproduce the zero-energy limit of the full two-body T matrix, giving $g = U_0 \Gamma$ where $U_0 = 4\pi\hbar^2 a/m$ and $\Gamma = (1 - 2a\Lambda/\pi)^{-1}$. In the $\Lambda \to \infty$ limit, $\hat{V}$ is equivalent to a renormalized contact potential; however, we do not take Λ arbitrarily large. In the spirit of Refs. [33–35], Λ is instead calibrated to reproduce finite-range corrections to the Feshbach molecule binding energy $-\hbar^2/m(a - \bar{a})^2$ away from unitarity where $\bar{a} = 0.955 r_{\mathrm{vdW}}$ is the mean-scattering length depending on the van der Waals length r_{vdW} for a particular atomic species [1,36] (see Supplemental Material [37] for ^{39}K and ^{85}Rb calibration). This yields $\Lambda = 2/\pi\bar{a}$, introducing finite-range effects into our many-body model, removing the need for an additional three-body parameter, and avoiding the unphysical Thomas collapse [38] in our calculation of Efimov clusters discussed below.

From Eq. (2), we use the Heisenberg equation of motion $i\hbar\dot{\hat{\mathcal{O}}} = [\hat{\mathcal{O}}, \hat{H}]$ and obtain the HFB equations for the dynamics of the first- and second-order cumulants

$$i\hbar\dot{\psi}_0 = g\left(|\zeta(0)|^2 |\psi_0|^2 + 2\sum_{\mathbf{k}\neq 0} |\zeta(\mathbf{k})|^2 \rho_{\mathbf{k}}\right)\psi_0 + g\psi_0^* \sum_{\mathbf{k}\neq 0} \zeta(0)\zeta^*(2\mathbf{k})\kappa_{\mathbf{k}}, \tag{3}$$

$$i\hbar\dot{\kappa}_{\mathbf{k}} = 2h(\mathbf{k})\kappa_{\mathbf{k}} + (1 + 2\rho_{\mathbf{k}})\Delta(\mathbf{k}), \tag{4}$$

$$\hbar\dot{\rho}_{\mathbf{k}} = 2\,\mathrm{Im}[\Delta(\mathbf{k})\kappa^*_{\mathbf{k}}], \tag{5}$$

where

$$h(\mathbf{k}) = \frac{\hbar^2 k^2}{2m} + 2g|\zeta(\mathbf{k})|^2|\psi_0|^2 + 2g\sum_{\mathbf{k}'\neq 0} |\zeta(\mathbf{k} - \mathbf{k}')|^2 \rho_{\mathbf{k}'}, \tag{6}$$

$$\Delta(\mathbf{k}) = g\zeta(2\mathbf{k})\left(\zeta^*(0)\psi_0^2 + \sum_{\mathbf{k}'\neq 0} \zeta^*(2\mathbf{k}')\kappa_{\mathbf{k}'}\right) \tag{7}$$

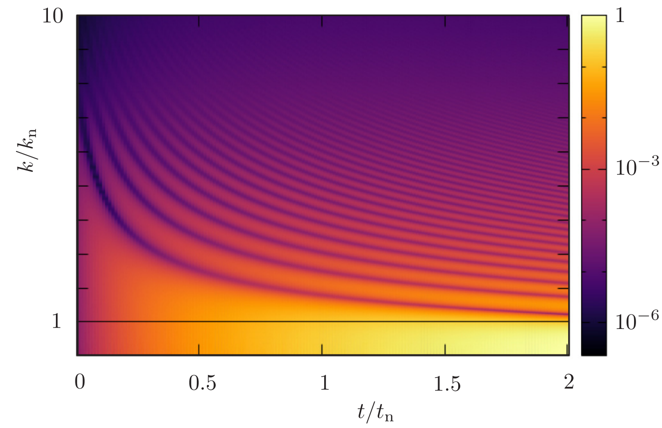

FIG. 1. Density plot of the universal excitation density $\rho_{\mathbf{k}}$ evolving at unitarity after a 5 μs quench. The "rippling" effect is due to ballistic correlation waves studied in Ref. [23]. The black line indicates the scale of the Fermi wave number k_{n} where excitation buildup is most pronounced. We find that $\rho_{\mathbf{k}} > 1$ for $t \gtrsim 2t_{\mathrm{n}}$ within our model.

are the Hartree-Fock Hamiltonian and pairing field, respectively [30]. At unitarity, $g = -\pi^3\hbar^2\bar{a}/m$ and we recover the full T matrix at resonance from the vacuum limit of Eq. (4) (see Ref. [37]). We mimic the initial quench sequence of Refs. [2–4] and ramp a pure Bose condensate onto resonance over the course of 5 μs and then evolve the system at unitarity. The HFB theory, Eqs. (3)–(5), describes the quantum depletion of a Bose condensate via the generation of correlated excitation pairs studied in Ref. [39]. The universal evolution of the excitation density $\rho_{\mathbf{k}}$ is shown in Fig. 1, where a decaying k^{-4} leading-order tail develops at high momentum proportional to the Tan contact [40–42]. This is due to the growth of two-body correlations at short distances $r \ll n^{-1/3}$ [39]. On the Fermi timescale, a macroscopic buildup of excitations occurs on the scale of k_{n}, indicated by the dashed line in Fig. 1, eventually violating the assumptions underlying our model as $\rho_{\mathbf{k}}$ exceeds unity. We find that this breakdown occurs universally after evolving a time $t \approx 2t_{\mathrm{n}}$ at unitarity.

Embedded few-body Schrödinger equations. Equations (3)–(5) describe the evolving many-body background up to second-order correlations. Using this description, we investigate the bound two- and three-body clusters formed within the depletion and introduce to the set of cumulant equations the triplet $\tau^{0,3}_{\mathbf{k},\mathbf{k}'} = \langle \hat{a}_{-\mathbf{k}-\mathbf{k}'} \hat{a}_{\mathbf{k}} \hat{a}_{\mathbf{k}'} \rangle_c$, where the superscript notation indicates the number of creation and annihilation operators, respectively. The inclusion of $\dot{\tau}^{0,3}_{\mathbf{k},\mathbf{k}'}$ into the hierarchy of cumulant equations has been proposed as a general starting point for including the Efimov effect, along with a broad range of unknown effects, into a many-body theory of the unitary Bose gas [43]. Unlike the embedded impurity problem, bound clusters in the unitary Bose-condensed gas are indistinguishable from the background and are therefore subject to Bose stimulation. The dynamics of $\kappa_{\mathbf{k}}$ and $\tau^{0,3}_{\mathbf{k},\mathbf{k}'}$, which include two- and three-body scattering in medium, generally occur on timescales shorter than the density dynamics [29,43]. Treating density effects as quasistationary, the principle portion of the cumulant equations for $\dot{\kappa}_{\mathbf{k}}$ and $\dot{\tau}^{0,3}_{\mathbf{k},\mathbf{k}'}$ defines eigenvalue equations

$$E_{2B}^{(\nu)}\phi_\nu(\mathbf{k}) = 2h(\mathbf{k})\phi_\nu(\mathbf{k}) + (1+2\rho_\mathbf{k})\sum_{\mathbf{k}'\neq 0} g\zeta(2\mathbf{k})\zeta^*(2\mathbf{k}')\phi_\nu(\mathbf{k}'), \tag{8}$$

$$E_{3B}^{(\nu)}\Psi_\nu(\mathbf{k},\mathbf{k}') = (1+\hat{P}_+ + \hat{P}_-)\left(h(\mathbf{k})\Psi_\nu(\mathbf{k},\mathbf{k}') + (1+\rho_{\mathbf{k}'}+\rho_{\mathbf{k}+\mathbf{k}'})\sum_{\mathbf{k}''\neq 0} g\zeta(2\mathbf{k}'+\mathbf{k})\zeta^*(2\mathbf{k}''+\mathbf{k})\Psi_\nu(\mathbf{k},\mathbf{k}'')\right), \tag{9}$$

where we have ignored inhomogeneities that describe scattering amongst clusters (see Ref. [37]). Iterative solution of Eqs. (8) and (9) yields two- and three-body cluster eigenenergies $E_{2B}^{(\nu)}$ and $E_{3B}^{(\nu)}$ and right-handed wave functions $\phi_\nu(\mathbf{k})$ and $\Psi_\nu(\mathbf{k},\mathbf{k}')$ evolving on the timescale of the many-body background [44]. This treatment is formally similar to the derivation of the hyperbolic Wannier equation [43], and both equations are bosonic analogs of the Wannier equation [29,45] describing bound electron-hole pairs in semiconductors. The operators $\hat{P}_-$, $\hat{P}_+$ indicate cyclic and anticyclic permutations, respectively. In the zero-density limit, Eqs. (8) and (9) reduce to the two- and three-particle Schrödinger equation, respectively, and therefore describe *embedded* extensions.

In the regime $\Lambda \gg \xi^{-1}$, where $\xi^2 = \hbar^2/2m|g|n$ is the condensate healing length [46], we find that $h(\mathbf{k}) \approx \hbar^2k^2/m + 2gn$, and the structure of Eqs. (8) and (9) simplifies. In our model at unitarity this limit is equivalent to the diluteness criterion $nr_{\mathrm{vdW}}^3 \ll 1$, which is well satisfied by all unitary degenerate Bose gas experiments to date ($nr_{\mathrm{vdW}}^3 < 10^{-5}$) [2–4]. Consequently, we report cluster binding energies $\tilde{E}_{2B}^{(\nu)} \equiv E_{2B}^{(\nu)} - 4gn$ and $\tilde{E}_{3B}^{(\nu)} \equiv E_{3B}^{(\nu)} - 6gn$ relative to the embedded two- and three-body continuum thresholds. Additionally, we define a nonsymmetric effective pairwise interaction $\hat{V}_{\mathrm{eff}} \equiv \hat{B}\hat{V}$ where $\langle\mathbf{k},\mathbf{k}'|\hat{B} = (1+\rho_\mathbf{k}+\rho_{\mathbf{k}'})\langle\mathbf{k},\mathbf{k}'|$ Bose-enhances collisions occurring in medium. On the Fermi timescale, the operator $\hat{B}$ enhances pairwise interactions disproportionately at the scale of the interparticle spacing, as shown in Fig. 1. This effect was first studied in Ref. [43] for a Bose-condensed gas of ^{85}Rb quenched to unitarity at density $nr_{\mathrm{vdW}}^3 = 2\times 10^{-7}$ and evolution time $t \sim 800$ μs, observing a 528 Hz ($\approx 0.3E_\mathrm{n}$) blueshift in the binding energy of the resonant two-body bound state [47]. In this work, we present a systematic study of the evolution of two- and three-body bound clusters in the unitary regime over a range of densities.

Two-body bound clusters. To study bound two-body clusters, we reformulate the embedded two-body Schrödinger equation, Eq. (8), as a Lippman-Schwinger equation for the embedded two-body T operator $\hat{\mathcal{T}}_{2B}(z) = \hat{B}\hat{V} + \hat{B}\hat{V}\hat{G}_{2B}^{(0)}(z)\hat{\mathcal{T}}_{2B}(z)$, where $\hat{G}_{2B}^{(0)}(z) \equiv (z-2\hat{t})^{-1}$ is the two-body free Green's operator with kinetic energy operator $\hat{t}|\mathbf{k}\rangle = \hbar^2k^2/2m|\mathbf{k}\rangle$ and energy z relative to the embedded two-body continuum threshold (see Ref. [37]). Our $\hat{\mathcal{T}}_{2B}(z)$ is related to the "many-body T operator" $\hat{B}\hat{T}_{\mathrm{MB}}(z) = \hat{\mathcal{T}}_{2B}(z)$ introduced in Ref. [48], which predicts weakly bound pairs at unitarity in the finite temperature phase diagram of the strongly interacting Bose gas [49]. For separable potentials, we obtain the closed expression for the full embedded two-body T operator

$$\hat{\mathcal{T}}_{2B}(z) = \hat{B}\frac{g|\zeta\rangle\langle\zeta|}{1-g\langle\zeta|\hat{G}_{2B}^{(0)}(z)\hat{B}|\zeta\rangle}. \tag{10}$$

The position of the simple pole in Eq. (10) corresponds to the dimer binding energy of a two-body cluster $z = \tilde{E}_{2B}^{(\mathrm{D})}$, with wave function $|\phi_\mathrm{D}\rangle \propto \hat{G}_{2B}^{(0)}(\tilde{E}_{2B}^{(\mathrm{D})})\hat{B}|\zeta\rangle$.

To parametrize the binding energy and size of the two-body bound cluster, we define an effective two-body scattering length $-\hbar^2/ma_{\mathrm{eff}}^2 \equiv \tilde{E}_{2B}^{(\mathrm{D})}$. Over a range of densities and times shown in Fig. 2, we find that a_{eff} scales continuously solely with the density quantified by the dynamical scaling power law

$$\tilde{E}_{2B}^{(\mathrm{D})} = -E_\mathrm{n}\left[1.12 + 2.43\left(\frac{t_\mathrm{n}}{t}\right)^2\right]^{-2}. \tag{11}$$

This fitted equation matches the universal binding energy $\tilde{E}_{2B}^{(D)} \approx -0.3E_\mathrm{n}$ found at the latest time considered in our model $t \approx 2t_\mathrm{n}$ and predicts the universal asymptotic binding energy $\tilde{E}_{2B}^{(\mathrm{D})} \approx -0.8E_\mathrm{n}$. Due to the minimal amount of quantum depletion during the quench, the two-body bound cluster is initially nearly resonant $k_\mathrm{n}a_{\mathrm{eff}} \sim 10^3$ with the embedded

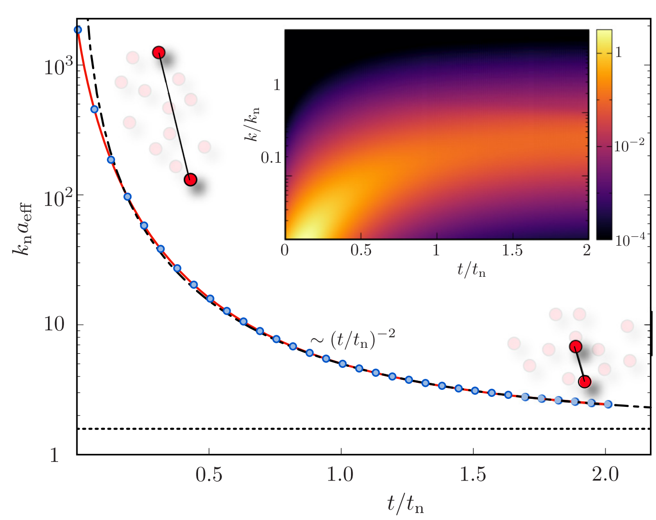

FIG. 2. Evolution of a_{eff} for two densities within the range of experimental interest, $nr_{\mathrm{vdW}}^3 = 10^{-7}$ (solid red curve) and 10^{-9} (blue data points). The fitted universal result in Eq. (11) corresponds to the dash-dotted black line with asymptotic estimate $a_{\mathrm{eff}} = 0.41n^{-1/3}$ (dotted black line). The inset shows a density plot of the universal dynamics of the two-body bound cluster probability density $k^2|\phi_\mathrm{D}(\mathbf{k})|^2/(1+2\rho_\mathbf{k})$ in arbitrary units [44].

two-body scattering threshold as shown in Fig. 2. Quantum depletion on the Fermi timescale enhances pairwise interactions at the scale of k_n shown in Fig. 1, and $\hat{V}_{\text{eff}}$ supports a universal two-body cluster bound entirely by many-body effects. Consequently, the extended two-body bound cluster shrinks to the asymptotic prediction $a_{\text{eff}} = 0.41n^{-1/3}$ of Eq. (11). The dynamic localization of the universal bound two-body cluster towards the scale of the interparticle spacing is shown in the inset of Fig. 2.

Three-body bound clusters. In vacuum it is well-known that the shallow two-body bound state for $a > 0$ is associated with a finite set of Efimov states, merging sequentially with the atom-molecule threshold as a is decreased from unitarity [50]. Analogously, the dynamical formation of the universal bound two-body cluster and coincident decrease of a_{eff} must also have consequences for the spectrum of Efimov clusters.

To study these effects, we decompose the three-body wave function into Faddeev components $|\Psi_\nu\rangle = (1 + \hat{P}_+ + \hat{P}_-)|\Psi_\nu^{(1)}\rangle$, obeying the bound-state Faddeev equation $|\Psi_\nu^{(1)}\rangle = \hat{G}_{3\text{B}}^{(0)}(z)\hat{\mathcal{T}}_{23}(z)(\hat{P}_+ + \hat{P}_-)|\Psi_\nu^{(1)}\rangle$ [31] where $\hat{\mathcal{T}}_{23}(z) = \hat{B}_1\hat{V}_1 + \hat{B}_1\hat{V}_1\hat{G}_{3\text{B}}^{(0)}(z)\hat{\mathcal{T}}_{23}(z)$, and the energy z is defined relative to the embedded three-body continuum threshold. Here we have used the spectator notation to indicate pairwise interaction between atoms 2 and 3 and defined the three-body free Green's operator, $\hat{G}_{3\text{B}}^{(0)}(z) \equiv (z - \sum_{i=1}^{3}\hat{t}_i)^{-1}$. Following the original formulation of Skorniakov and Ter-Martirosian [51], we make the ansatz $|\Psi_\nu^{(1)}\rangle \propto \hat{G}_{3\text{B}}^{(0)}(\tilde{E}_{3\text{B}}^{(\nu)})\hat{B}_1(|\zeta\rangle \otimes |\mathcal{F}_\nu\rangle)$. The tensor product is defined as $\langle \mathbf{q}_1, \mathbf{p}_1|(|\zeta\rangle \otimes |\mathcal{F}_\nu\rangle) = \zeta(2q_1)\mathcal{F}_\nu(p_1)$ in terms of the Jacobi vectors $\mathbf{q_1} = (\mathbf{k_2} - \mathbf{k_3})/2$ and $\mathbf{p_1} = (2\mathbf{k_1} - \mathbf{k_2} - \mathbf{k_3})/3$. Inserting this ansatz into Eq. (9) yields the integral equation for the amplitude

$$\mathcal{F}_\nu(p_1) = 2g\tau\left(\tilde{E}_{3\text{B}}^{(\nu)} - \frac{3\hbar^2 p_1^2}{4m}\right)\int \frac{d^3p'}{(2\pi)^3}\,(1 + \rho_{\mathbf{p_1}} + \rho_{\mathbf{p_1+p'}}) \times \frac{\zeta(|2\mathbf{p_1} + \mathbf{p}'|)\zeta(|2\mathbf{p}' + \mathbf{p}'|)}{\tilde{E}_{3\text{B}}^{(\nu)} - \frac{\hbar^2}{m}\left(p_1^2 + p'^2 + \mathbf{p_1}\cdot\mathbf{p}'\right)}\mathcal{F}_\nu(p'), \qquad (12)$$

where $\tau(z) = 1/(1 - g\langle\zeta|\hat{G}_{2\text{B}}^{(0)}(z)\hat{B}|\zeta\rangle)$. At unitarity, nontrivial solutions of Eq. (12) for negative energies correspond to the spectrum of Efimov clusters [37].

Solving Eqs. (10) and (12), we obtain the evolution of two-body and Efimov cluster binding energies over a range of densities shown in Fig. 3, where scaling laws are apparent. Over the time range considered, the two-body bound cluster binding energy scales continuously as a density power law $n^{2/3}$. At early times ($t \ll t_{\text{n}}$), however, the ground, first, and second-excited Efimov cluster binding energies $\tilde{E}_{3\text{B}}^{(0)}$, $\tilde{E}_{3\text{B}}^{(1)}$, and $\tilde{E}_{3\text{B}}^{(2)}$, respectively, are insensitive to density variations, displaying the intrinsic discrete scaling of Efimov states in vacuum with the van der Waals energy $E_{\text{vdW}} = \hbar^2/mr_{\text{vdW}}^2$. The initial Efimov cluster spectrum is $|\tilde{E}_{3\text{B}}^{(\nu)}| = e^{-2\pi\nu/s_0}\hbar^2\kappa_*^2/m$, where κ_* is the three-body parameter $\kappa_* \approx 0.211/r_{\text{vdW}}$ [52,53].

As the unitary Bose gas forms on the Fermi timescale, Efimov clusters become increasingly sensitive to the background buildup of pairing excitations at the scale of the interparticle spacing. Generally, Efimov clusters must be more bound than the embedded atom-molecule threshold at energy $\tilde{E}_{2\text{B}}^{(\text{D})}$

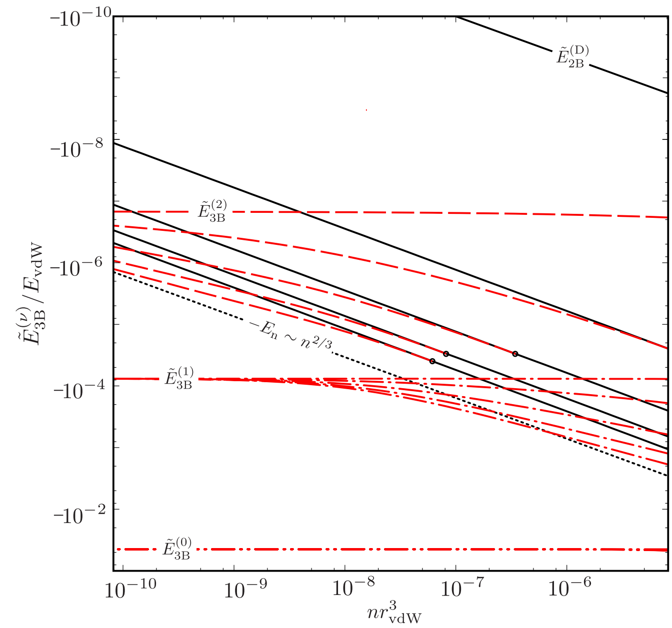

FIG. 3. Universal two-body (solid black curve) and Efimov cluster (dashed and dashed-dotted red curves) binding energies over a range of evolution times at unitarity and densities of experimental interest. For a given bound cluster, evolution in time is denoted by increasingly negative binding energies from $0, 0.5t_{\text{n}}, \ldots, 2t_{\text{n}}$. The circled data points indicate the absorption of an Efimov cluster into the embedded atom-molecule threshold. The log-log scale reveals the scaling behavior of the energies with the atomic density and the Fermi energy (dotted black curve).

relative to the embedded three-body continuum. In Fig. 3, we see that Efimov clusters sensitive to these scales become progressively localized as their binding energies are blueshifted. Consequently, Efimov clusters scale continuously with the $n^{2/3}$ power law over a range of atomic densities. This behavior persists until a blueshifted Efimov cluster is either absorbed into the embedded atom-molecule scattering continuum or a_{eff} approaches its asymptotic limit as the gas equilibrates. This process is repeated log-periodically for densities separated by powers of $e^{3\pi/s_0} \approx 22.7^3$. Over the density range of experimental interest, the ground-state Efimov cluster energy in Fig. 3, however, remains insensitive to both density variation and evolution at unitarity due to its relative localization.

The absorption of an Efimov cluster into the embedded atom-molecule scattering continuum is analogous to the behavior of the vacuum Efimov state spectrum for decreasing $a > 0$ [32,54], and therefore we expect this dynamical process to be *sequential.* Although only the first three Efimov clusters are shown in Fig. 3, our results confirm this behavior also for highly excited Efimov clusters. Quantitatively, we estimate absorption times for the excited Efimov clusters at a given density

$$\frac{t^{(\nu)}(n)}{t_{\text{n}}} = [-0.461 + (0.093 \pm 0.007)r_{\text{vdW}}k_{\text{n}}e^{\nu\pi/s_0}]^{-1/2}, \qquad (13)$$

where the uncertainty is due to the finite time step of our many-body simulation [37]. To make Eq. (13) well defined, we restrict the domain of $t^{(\nu)}(n)$ to densities above $n^{(\nu)}r_{\rm vdW}^3 = (2.12 \pm 0.45)e^{-3\pi\nu/s_0}$, where $t^{(\nu)}(n^{(\nu)})/t_{\rm n} \to \infty$. For densities below $n^{(\nu)}$, our results indicate that the νth Efimov cluster remains permanently in the bound-cluster spectrum. Furthermore, Eq. (13) predicts that increasingly highly excited Efimov trimers are absorbed exponentially faster, leaving only a finite number of Efimov clusters on the Fermi timescale. Due also to the minimal amount of quantum depletion occurring during the quench, $a_{\rm eff}$ is initially finite as shown in Fig. 2, and there is a finite set of Efimov clusters before the sequential absorption commences.

Conclusion. By systematically applying the cumulant expansion, we have developed a time-dependent picture of the bound cluster composition of the quenched unitary Bose gas. The size of the dynamically formed unitary two-body clusters is given by the length scale $a_{\rm eff}$, which reduces within a few Fermi times to a value proportional to the interparticle spacing. As this cluster size governs three-body recombination, it gives rise to a universal per-particle loss rate scaling as $n^2 a_{\rm eff}^4 \propto n^{2/3}$, qualitatively matching the scaling behavior observed experimentally [3,4]. Analyzing this pathway for three-body recombination remains the subject of future studies. The appearance of Efimov clusters in the spectrum of $\tau^{0,3}_{\mathbf{k},\mathbf{k}'}$ reveals a straightforward extension of the cumulant equations to include Efimov physics in the many-body theory of the unitary Bose gas. Prospects for observing the two- and three-body cluster binding energies through time-resolved rf spectroscopy performed at unitarity [55–57] might be challenging due to loss timescales. Alternatively, by sweeping the interaction strength away from unitarity, the dynamical projection of bound clusters onto final-state molecules may be studied theoretically to analyze the experimental results of Refs. [3,4], although this is left for future study. The sensitivity of Efimov clusters to the background buildup of excitations on Fermi timescales may also be experimentally observable as an oscillation chirp of the three-body Tan contact predicted in Ref. [24]. Away from unitarity, the study of embedded few-body Schrödinger equations may also provide insight into the structure of other systems with substantial quantum depletion [58,59].

Acknowledgments. The authors thank José D'Incao, Murray Holland, John Corson, Paul Mestrom, and Thomas Secker for fruitful discussions. This work is supported by Netherlands Organisation for Scientific Research (NWO) under Grant No. 680-47-623.

[1] C. Chin, R. Grimm, P. Julienne, and E. Tiesinga, Rev. Mod. Phys. **82**, 1225 (2010).
[2] P. Makotyn, C. E. Klauss, D. L. Goldberger, E. Cornell, and D. S. Jin, Nat. Phys. **10**, 116 (2014).
[3] C. E. Klauss, X. Xie, C. Lopez-Abadia, J. P. D'Incao, Z. Hadzibabic, D. S. Jin, and E. A. Cornell, Phys. Rev. Lett. **119**, 143401 (2017).
[4] C. Eigen, J. A. P. Glidden, R. Lopes, N. Navon, Z. Hadzibabic, and R. P. Smith, Phys. Rev. Lett. **119**, 250404 (2017).
[5] T. Schäfer and D. Teaney, Rep. Prog. Phys. **72**, 126001 (2009).
[6] C. Chin, in *Universal Themes of Bose-Einstein Condensation*, edited by N. P. Proukakis, D. W. Snoke, and P. B. Littlewoo (Cambridge University Press, Cambridge, UK, 2017), Chap. 9, pp. 168–186.
[7] K. M. Hara, S. L. Hemmer, M. E. Gehm, S. R. Granade, and J. E. Thomas, Science **298**, 2179 (2002).
[8] C. Cao, E. Elliott, J. Joseph, H. Wu, J. Petricka, T. Schäfer, and J. E. Thomas, Science **331**, 58 (2011).
[9] T.-L. Ho, Phys. Rev. Lett. **92**, 090402 (2004).
[10] V. Efimov, Sov. J. Nucl. Phys. **12**, 101 (1971).
[11] V. Efimov, Sov. J. Nucl. Phys. **29**, 546 (1979).
[12] P. Naidon, J. Phys. Soc. Jpn. **87**, 043002 (2018).
[13] M. Sun, H. Zhai, and X. Cui, Phys. Rev. Lett. **119**, 013401 (2017).
[14] S. M. Yoshida, S. Endo, J. Levinsen, and M. M. Parish, Phys. Rev. X **8**, 011024 (2018).
[15] N. T. Zinner, Europhys. Lett. **101**, 60009 (2013).
[16] L. A. Peña Ardila and S. Giorgini, Phys. Rev. A **92**, 033612 (2015).
[17] X. Qiu, X. Cui, and W. Yi, Phys. Rev. A **94**, 051604 (2016).
[18] N. G. Nygaard and T. Z. Nikolaj, New J. Phys **16**, 023026 (2014).
[19] C. J. M. Mathy, M. M. Parish, and D. A. Huse, Phys. Rev. Lett. **106**, 166404 (2011).
[20] D. J. MacNeill and F. Zhou, Phys. Rev. Lett. **106**, 145301 (2011).
[21] S. Endo, A. M. García-García, and P. Naidon, Phys. Rev. A **93**, 053611 (2016).
[22] Y. Nishida, Phys. Rev. Lett. **114**, 115302 (2015).
[23] J. P. Corson and J. L. Bohn, Phys. Rev. A **94**, 023604 (2016).
[24] V. E. Colussi, J. P. Corson, and J. P. D'Incao, Phys. Rev. Lett. **120**, 100401 (2018).
[25] J. P. D'Incao, J. Wang, and V. E. Colussi, Phys. Rev. Lett. **121**, 023401 (2018).
[26] C. Klauss, Resonantly Interacting Degnerate Bose Gas Oddities, Ph.D. thesis, University of Colorado, 2017.
[27] U. Eismann, L. Khaykovich, S. Laurent, I. Ferrier-Barbut, B. S. Rem, A. T. Grier, M. Delehaye, F. Chevy, C. Salomon, L.-C. Ha, and C. Chin, Phys. Rev. X **6**, 021025 (2016).
[28] T. Köhler and K. Burnett, Phys. Rev. A **65**, 033601 (2002).
[29] M. Kira and S. W. Koch, *Semiconductor Quantum Optics* (Cambridge University Press, Cambridge, UK, 2011).
[30] J.-P. Blaizot and G. Ripka, *Quantum Theory of Finite Systems*, Vol. 3 (MIT, Cambridge, MA, 1986).
[31] L. D. Faddeev and S. P. Merkuriev, *Quantum Scattering Theory for Several Particle Systems* (Springer Science & Business Media, Berlin, 2013), Vol. 11.
[32] P. Naidon and S. Endo, Rep. Prog. Phys. **80**, 056001 (2017).
[33] S. J. J. M. F. Kokkelmans and M. J. Holland, Phys. Rev. Lett. **89**, 180401 (2002).
[34] M. D. Lee, T. Köhler, and P. S. Julienne, Phys. Rev. A **76**, 012720 (2007).
[35] M. Stoll and T. Köhler, Phys. Rev. A **72**, 022714 (2005).
[36] G. F. Gribakin and V. V. Flambaum, Phys. Rev. A **48**, 546 (1993).

[37] See Supplemental Material at http://link.aps.org/supplemental/10.1103/PhysRevA.98.051601, which includes Refs. [60–66], for additional details of our calculations.
[38] L. H. Thomas, Phys. Rev. **47**, 903 (1935).
[39] A. G. Sykes, J. P. Corson, J. P. D'Incao, A. P. Koller, C. H. Greene, A. M. Rey, K. R. A. Hazzard, and J. L. Bohn, Phys. Rev. A **89**, 021601 (2014).
[40] S. Tan, Ann. Phys. (NY) **323**, 2952 (2008).
[41] S. Tan, Ann. Phys. (NY) **323**, 2971 (2008).
[42] S. Tan, Ann. Phys. (NY) **323**, 2987 (2008).
[43] M. Kira, Ann. Phys. (NY) **356**, 185 (2015).
[44] Nonsymmetric eigenvalue problems have both left- and right-handed eigenvectors. By inspection the two and three-body left-handed wave functions are $\langle\phi_\nu^{(L)}| = \langle\phi_\nu|\hat{B}^{-1}$ and $\langle\Psi_\nu^{(L)}| = \langle\Psi_\nu|[\hat{B}_1(1+\hat{P}_+ + \hat{P}_-)]^{-1}$, respectively. These eigenfunctions can be normalized as $\sum_{\mathbf{k}}[\phi_\nu^{(L)}(\mathbf{k})]^*\phi_{\nu'}(\mathbf{k}) = \delta_{\nu,\nu'}$ and $\sum_{\mathbf{k},\mathbf{k}'}[\Psi_\nu^{(L)}(\mathbf{k},\mathbf{k}')]^*\Psi_{\nu'}(\mathbf{k},\mathbf{k}') = \delta_{\nu,\nu'}$.
[45] G. H. Wannier, Phys. Rev. **52**, 191 (1937).
[46] E. P. Gross, J. Math. Phys. **4**, 195 (1963).
[47] We note that the result of Refs. [43,67] account for third- and higher-order cumulant effects phenomenologically.
[48] H. T. C. Stoof, M. Bijlsma, and M. Houbiers, J. Res. Natl. Inst. Stand. Technol. **101**, 443 (1996).
[49] A. Koetsier, P. Massignan, R. A. Duine, and H. T. C. Stoof, Phys. Rev. A **79**, 063609 (2009).
[50] E. Braaten and H.-W. Hammer, Ann. Phys. (NY) **322**, 120 (2007).
[51] G. V. Skorniakov and K. A. Ter-Martirosian, Zh. Eksp. Teor. Fiz. **31**, 775 (1956).
[52] J. Wang, J. P. D'Incao, B. D. Esry, and C. H. Greene, Phys. Rev. Lett. **108**, 263001 (2012).
[53] P. Naidon, S. Endo, and M. Ueda, Phys. Rev. A **90**, 022106 (2014).
[54] J. P. D'Incao, J. Phys. B: At., Mol. Opt. Phys. **51**, 043001 (2018).
[55] A. B. Bardon, S. Beattie, C. Luciuk, W. Cairncross, D. Fine, N. S. Cheng, G. J. A. Edge, E. Taylor, S. Zhang, S. Trotzky, and J. H. Thywissen, Science **344**, 722 (2014).
[56] R. J. Wild, P. Makotyn, J. M. Pino, E. A. Cornell, and D. S. Jin, Phys. Rev. Lett. **108**, 145305 (2012).
[57] O. Machtey, Z. Shotan, N. Gross, and L. Khaykovich, Phys. Rev. Lett. **108**, 210406 (2012).
[58] E. A. Donley, N. R. Claussen, S. L. Cornish, J. L. Roberts, E. A. Cornell, and C. E. Wieman, Nature (London) **412**, 295 (2001).
[59] K. Xu, Y. Liu, D. E. Miller, J. K. Chin, W. Setiawan, and W. Ketterle, Phys. Rev. Lett. **96**, 180405 (2006).
[60] T. Secker (private communication).
[61] E. A. Donley, N. R. Claussen, S. T. Thompson, and C. E. Wieman, Nature (London) **417**, 529 (2002).
[62] C. D'Errico, M. Zaccanti, M. Fattori, G. Roati, M. Inguscio, G. Modugno, and A. Simoni, New J. Phys. **9**, 223 (2007).
[63] N. P. Proukakis and K. Burnett, J. Res. Natl. Inst. Stand. Technol. **101**, 457 (1996).
[64] A. Rançon and K. Levin, Phys. Rev. A **90**, 021602 (2014).
[65] J. R. Taylor, *Scattering Theory: The Quantum Theory of Nonrelativistic Collisions* (Courier Corporation, North Chelmsford, 2006).
[66] W. H. Press, B. P. Flannery, S. A. Teukolsky, and W. T. Vetterling, *Numerical Recipes* (Cambridge University Press, Cambridge, 1989), Vol. 3.
[67] M. Kira, Nat. Commun. **6**, 6624 (2015).